GFRP REINFORCING OF CONCRETE MASONRY INFILL WALLS

Wael W. El-Dakhakhni, Drexel University, Philadelphia, PA, USA
Ahmad A. Hamid, Drexel University, Philadelphia, PA, USA
Mohamed Elgaaly, Drexel University, Philadelphia, PA, USA

Abstract

Masonry infill walls in frame structures have been long known to affect the strength and stiffness of the infilled frame structures. In seismic areas, ignoring the composite action is not always on the safe side, since the interaction between the wall and the frame under lateral loads dramatically changes the dynamic characteristics of the composite structure and hence its response to seismic loads. It has been generally recognized that infill walls enhance the response of frame buildings in low to moderate seismic regions, yet they exhibit poor seismic performance under high seismic demand. This behavior is due to the degradation of stiffness, strength and energy dissipation capacity, which results from the progressive damage of the masonry wall and the deterioration of the wall-frame interfaces. Due to the difficulty associated with modeling, attempts of isolating the infill wall from the surrounding frame have been suggested. These attempts faced failure, primarily because of the out-of-plane instability associated with these techniques. This paper presents an ongoing study on the reinforcing of concrete masonry infill walls using GFRP laminates. Preliminary results of the study showed that the GFRP enhanced the system behavior under high loads and prevented undesirable failure modes. The GFRP reinforcing technique would also facilitate modeling by means of eliminating the anisotropic nature of masonry walls and clearly defining the failure mode of the reinforced system.

Introduction

Masonry infill walls can be found as interior partitions or exterior facades in reinforced concrete and steel frame structures. Since they are normally considered as architectural elements, their presence is often ignored by structural engineers. However, they tend to interact with the surrounding frame when the structure is subjected to wind or earthquake loads; the resulting system is referred to as an *infilled frame*. Ignoring the effect of infill walls in designing new buildings and relying on it in analysis of existing ones for upgrading and retrofitting purposes is not the right, yet it is the easiest approach. This approach is not always conservative, and whether the inclusion of infill walls is conservative or not in the analysis depends, among many factors, on the site where the building is located. This effect is shown in Fig. 1, where T_{if} is the initial period of vibration of the infilled frame, and T_{bf} is the initial period of vibration of the bare frame, for an earthquake having a response spectrum following curve A, the total base shear on the bare structure could increase. Alternatively, for earthquake B, the base shear would decrease because of the addition of the infill walls.

The ongoing study at Drexel University presents a proposed design methodology of reinforcing concrete masonry-infilled steel frame (CMISF) structures using glass fiber-reinforced polymer (GFRP) laminates in order to enhance their seismic response. The reinforcing technique using GFRP laminates aims at creating an *engineered infill wall* with well defined stiffness and ultimate load capacity, by means of eliminating undesirable behavior and failure modes.

GFRP Contribution to the Response of Infilled Steel Frames

A preliminary experimental study using $^1/_3$ scale diagonally loaded square CMISF models was conducted at Drexel University [1].The study showed that the application of a GFRP laminate on the small scale masonry walls, has changed the stiffness, the ultimate load capacity, as well as the ductility of CMISF. Two different square steel frames with different sections were tested with similar $^1/_3$ scale masonry infill walls and the same type of GFRP laminate. The first frame, designated with the number 1, was composed of S335.7 sections and the frame sides measured 1.18 m center to center. The second frame, designated with the number 2, was composed of W6315 sections and the frame sides measured 1.26 m center to center . The slight difference in dimensions was designed to accommodate the same infill wall for the two frames. Table 1 summarizes the results of the tests, where, P_u is the ultimate load capacity; K_{in} is the initial secant stiffness determined from the load-deflection curve of the tested frames, defined as the slope of the line joining the two points at 5% and 50% of P_u.

As a first interpretation from Table 1, the GFRP reinforcing increased the strength of the unreinforced system by 110% for frame 1, and by 22% for frame 2. The increase in stiffness, however, was 135% and 92% for frames 1 & 2, respectively. It is also interesting to note that the infill wall, by itself, increased the strength of the bare frame by 267% for the first frame, yet with no significant increase for the second frame. A better way of looking at theses results would be to *isolate* the effect of the infill wall from the composite system; this is achieved by isolating both the stiffening and strengthening effects of the wall for both frames. In order to visualize this, refer to Figs. 2 and 3 for frames 1 & 2, respectively. In these figures, the suffixes **B**, **I**, and **R**, refer to **B**are, **I**nfilled, and **R**etrofitted frames respectively. The infill wall's share in the initial secant stiffness of the system is determined by subtracting the initial stiffness of the bare frame from that of the composite system, assuming that the two load-deflection curves are linear in their respective initial portions. As shown in Figs. 2 and 3, the strengthening effect, ΔP_u , of the wall is isolated by subtracting the bare frame load at the deflection level of which the failure of the composite system occurs as shown in the load-deflection behavior of frames 1 & 2, respectively. While the isolation of the wall effect for frame I-1 is an easy task, (since the bare frame, B-1, is much weaker than the composite I-1 frame), yet, further investigation is needed to isolate the wall effect in the I-2 frame. This is due to the fact that frame B-2 in much stronger than B-1 and its ultimate strength is comparable to the ultimate strength of I-2, yet under different ultimate deflections. In fact the infill wall fails first, then the steel frame picks up the majority of the applied load with smaller share of the infill wall. This is also apparent from the fact that the infill had a share in increasing the initial stiffness, yet due to its limited ductility compared to the steel frame, it failed prior to the frame reaching its ultimate strength. Table 1 gives the isolated wall's effect in increasing the stiffness and the strength for both the unreinforced as well as the reinforced frames, where, ΔP_u is the infill wall share of the ultimate load capacity at failure of the composite system; ΔK_{in} is the infill wall's share in the initial secant stiffness of the system.

From Table 1, it can be seen that, the reinforcing using the GFRP laminate increased the infill wall's stiffness by about 130% (143% for R-1 and 117% for R-2) and increased the wall's strength also by about 113% (126% for R-1 and 100% for R-2) of their respective unreinforced values. Although the infill walls used in the two frames are of the same material properties and dimensions, yet as apparent from Table 1, their stiffness and strength contribution in the two frames are not the same. This is attributed to the fact that the contact lengths between the wall and the frame, which in turn determines the effective width of the wall and hence its stiffness and strength is not the same for both frames. In

fact, the stiffer the frame, as it is the case of frame 2, the more the contact length between the frame and the wall, and hence the more the stiffness and the strength of the wall.

In short, the infilling effect, and consequently the reinforcing effect, depends on the load-deflection characteristics for both constituent of the composite system, namely, the steel frame and the infill wall. The infill reinforcing technique enhances the system ductility and eliminates the undesirable failure modes of the infill wall along with the uncertainty associated with them. The reinforcing, also, facilitates modeling of the wall by minimizing the anisotropy effect of masonry.

Conceptual Design of GFRP Reinforced Masonry Infill Walls

Based on the knowledge gained from both analytical and experimental studies during the last five decades [2 ,3], different failure modes of masonry-infilled frames were observed. The two most common modes are:

1. Corner crushing mode (*CC mode*), represents crushing of the infill in at least one of its loaded corners, as shown in Fig. 4-a. This mode is usually associated with infill of weak masonry blocks surrounded by a frame with weak joints and strong members.
2. Sliding shear mode (*SS mode*), represents horizontal sliding shear failure through bed joints of a masonry infill, as shown in Fig. 4-b. This mode is associated with infill of weak mortar joints and frame with strong members and joints.

The process of investigating all possible failure modes including the aforementioned two modes is a tedious task to determine which is the governing mode and consequently the governing failure load, *the supply*, to meet a certain *demand*. Hence the GFRP reinforcement scheme suggested herein seems like an optimum solution, since, if properly designed, the GFRP laminate should reduce the uncertainty in behavior, and suppress, as much as possible, the brittle behavior of masonry walls. This would result in reducing the seismic hazard associated with failure and in simplifying the modeling process.

The effect of the proposed reinforcement technique is of three different aspects, namely:

1. Preventing undesirable, *SS* brittle failure mode, which will result in reducing the P-Δ effect and the sudden drift associated with this mode. This is achieved by limiting all the possible failure modes to the *CC* mode, with well defined strength, stiffness and ductility. This, in turn, will result in eliminating the uncertainty associated with the modeling process.
2. Eliminating the anisotropic behavior of masonry, [4], by eliminating the shear-compression interaction in the mortar joints. This will transform the anistropic masonry wall into an orthotropic wall. Hence, modeling will be much easier.
3. Preventing out-of-plane failure or spalling of masonry blocks, which is, by itself, a major source of seismic hazard.

Isolation of the Reinforcing Technique Effects

Masonry infill walls have long been known to act as a diagonal strut connecting the two loaded corners. this assumption has been verified by different researchers in the last five decades [2, 3].

Since all the reinforced and the unreinforced infill walls failed in the corner crushing mode with no shear failure, and because of its practicality and ease of implementation in analysis, the diagonal strut concept will be utilized herein to present a method of analysis of CMISF reinforced with GFRP.
The increase in stiffness can be investigated by applying the diagonal strut concept, that is the wall is acting as a diagonal strut connecting the two loaded corners. The axial stiffness of the strut, K, is

$$K = \frac{E\ A}{L} \tag{1}$$

where, E, A and L are Young's Modulus, area and length of the strut, respectively. Since L remains unchanged with the reinforcement process, then it must be A and/or E which will change with reinforcing.
The increase in strength can be investigated also by applying the diagonal strut theory, that is the strength of the strut, F , is

$$F = \sigma\ A \tag{2}$$

where, σ is the ultimate compressive strength of the strut. Again, this means that σ and/or A which will change with reinforcement . In order to isolate the effect of each factor in increasing the stiffness and the strength of the infill the following design parameters are proposed:

1.The ω_d parameter describing the direct increase in the cross sectional area of the wall due to the inclusion of the GFRP laminate is defined as

$$\omega_d = \frac{A_{GFRP} + A_m}{A_m} \tag{3-a}$$

where, A_{GFRP}, and A_m are the GFRP and the masonry wall cross sectional areas, respectively.
In the common case of face shell mortar bedding, ω_d is defined as

$$\omega_d = \frac{t_{GFRP} + t_m}{t_m} \tag{3-b}$$

where, t_{GFRP}, is the GFRP laminate thickness, and t_m is the masonry wall face shell thickness. This parameter usually ranges between 1.05 and 1.15 .

2.The $\omega_{E\text{-}0}$, and $\omega_{E\text{-}90}$ parameters describing the increase in Young's modulus of the wall in the direction parallel and normal to the bed joints is defined respectively as

$$\omega_{E-0} = \frac{E_{r-0}}{E_{u-0}}\ ,\quad \omega_{E-90} = \frac{E_{r-90}}{E_{u-90}} \tag{4-a,b}$$

where, the suffixes r and u refer to reinforced and unreinforced masonry wall, respectively. These parameters were found to be ranging between 1.20 and 1.40 .

3.The ω_σ parameter giving the ratio between the compressive strength of the reinforced wall f'_{r-90}, to the unreinforced masonry wall strength f'_{u-90} in the direction normal to the bed joints is defined as

$$\omega_\sigma = \frac{f'_{r-90}}{f'_{u-90}} \tag{5}$$

This parameter was found to be ranging between 1.50 and 2.00 .

4.The ω_i parameter describing the indirect increase of the cross sectional area of the strut due to the fact that the GFRP laminate will force the wall to act as one unit, without diagonal cracks. This parameter is defined as

$$\omega_i = \frac{F_r}{F_u \times \omega_d \times \omega_\sigma} \tag{6}$$

where, F_r, and F_u are the reinforced and the unreinforced struts strength respectively.

5.The ω_μ parameter giving the displacement ductility ratio between the reinforced and the unreinforced infilled frames is defined as

$$\omega_\mu = \frac{\mu_r}{\mu_u} \tag{7}$$

where, μ_r, and μ_u are the reinforced and the unreinforced infilled frames ductility capacities respectively. In order to determine these design parameters, two levels of experimental work is currently being conducted by the authors at Drexel University. *Level I* is aimed at determining ω_d, ω_{E-0}, ω_{E-90}, ω_σ; and *Level II* for determining ω_i, ω_μ, as well as the energy dissipation and hysteretic properties of the reinforced infilled-frame system. As shown in Fig.5, *Level I* includes testing of compression prism specimens in both directions, parallel and normal to bed joints. It also includes testing specimens in direct shear and diagonal tension. For all these specimens, different configurations of GFRP are adopted in order to study the effect of the fiber orientation, the number of layers, and different reinforcement ratios on the reinforcing technique. *Level II* includes testing of full scale concrete masonry-infilled steel frames under quasi-static loading. The test matrix includes several parameters such as the effect of openings as well as the effect of using different GFRP configurations on the system behavior. The test setup for *Level II* is shown in Fig. 6. The following sections address the GFRP effect on defining the *CC* mode behavior after reinforcing and eliminating the *SS* failure mode by proper design of the laminate.

Design of GFRP to Eliminate the *SS* Mode

The *SS* mode is also relatively complicated to model, this is due to the *uncertainty* of the friction coefficient value between the mortar and the masonry blocks. Another factor is the complex shear-compression interaction in the wall's mortar joints.
The elimination of the *SS* mode, which causes the *knee brace* effect on the frame [5] is also of prime interest since it is a sudden, non-ductile mode of failure that causes severe damage to the frame columns.

It is also clear that due to the week bond strength of the mortar bed joints, (which will cause the *SS* mode), the full *CC* mode capacity of the wall would not be utilized.
The GFRP strength should be enough to prevent the *SS* mode to take place.
Due to a lateral load *H*, the maximum shear stress, τ_{max}, acting on the wall is

$$\tau_{max} = \frac{1.5H}{t_m l} \tag{8}$$

where *l* is the wall length. This equation is a simplification neglecting the principle stresses effect, which will result in a slight increase of this value when dealing with walls with common aspect ratios.
Hence the maximum shear force per unit length acting in the wall, q_{max}, will be

$$q_{max} = \frac{1.5H}{l} \tag{9}$$

It is then required by the reinforced bed joints to withstand this force in order to safeguard against developing the *SS* failure mode. The shear force supply per unit length at the bed joint, q_s, is

$$q_s = \tau_o \times t_m + \mu \frac{H \tan \theta}{l} + q_{GFRP} \tag{10}$$

An average value of the cohesive strength at the bed joints, $\tau_o = 0.03\ f9_{u\text{-}90}$, and the coefficient of friction $\mu = 0.3\text{-}1.2$, was suggested [5]. In this analysis, the cohesive strength will be neglected and the coefficient of friction will be taken conservatively as 0.3. Then, the shear force supply per unit length of the GFRP laminate, q_{GFRP} ,should be

$$q_{GFRP} = \frac{H}{l}\left[1.5 - 0.3 \tan\theta\right] \tag{11}$$

The GFRP shear strength depends on both the type as well as the orientation of the fibers within the GFRP laminate.

Modeling of GFRP Reinforced CMISF Failing in the CC Mode

Knowing the new composite material properties from Levels *I* and *II* experiments, the diagonal strut area and the effective compressive strength can be calculated based on available analytical models of CMISF. The reinforced strut ultimate load capacity, F_r, will be

$$F_c = A \times f'_{u-\theta} \times \omega_d \times \omega_\sigma \times \omega_i \tag{12}$$

where, $f9_{u\text{-}\theta}$, is the unreinforced masonry strength in the diagonal strut direction. The reinforced strut load capacity may be considered roughly twice that of the unreinforced as a first estimate or preliminary analysis purposes.

Modeling of CMISF which fails in the *CC* mode was under extensive studies in Drexel University [2, 3]. In these studies, the masonry wall was assumed to be orthotropic in the two principal directions, parallel and perpendicular to the bed joints, and the strut area, A, of the wall is

$$A = \frac{(1-\alpha_c)\alpha_c h\ t_m}{\cos\theta} \tag{13}$$

which generally ranges between 10% and 20% of the column height multiplied by the thickness of the wall, or twice the thickness of the face shells in case of face shell mortar bedding.
where, α_c is the ratio of the column contact length to the column height h, θ is defined as $\tan^{-1}\theta = (h/l)$, and l is the beam span. α_c was given by

$$\alpha_c h = \sqrt{\frac{2\ (M_{pj} + 0.2\ M_{pc})}{t_m f'_{u-0}}} \leq 0.4h \tag{14}$$

where, M_{pj} is the minimum of the column's, the beam's or the connection's plastic moment capacity, referred to as the plastic moment capacity of the joint, M_{pc} is the column plastic moment capacity, $f9_{u\text{-}0}$ is the compressive strength of the masonry wall parallel to the bed joint.

Due to the fact that the wall behaves as if it is *diagonally loaded*, the constitutive relations of orthotropic plates [6] can be used to obtain the Young's modulus, $E_{u\text{-}\theta}$, and the compressive strength of the wall in the diagonal direction, $f9_{u\text{-}\theta}$.
For the case of face shell bedding in hollow concrete masonry walls, it is suggested [3] to reduce both Young's modulus and the compressive strength of masonry in the direction normal to the bed joint by 15% in order to obtain those in the diagonal strut direction, i.e.

$$f'_{u-\theta} \cong 0.85 f'_{u-90} \tag{15}$$

CONCLUSIONS

The following conclusions resulted from the investigation:

1. The GFRP reinforcing technique enhances the infilled frame stiffness, strength, and ductility. The reinforcing effect depends on the load-deflection characteristics of both the steel frame and the reinforced infill panel and not the panel by itself.
2. The technique eliminates undesirable shear failure mode along with the uncertainties associated with its evaluation. The technique also facilitates modeling of the panel by minimizing the anisotropic behavior of masonry due to the weak shear strength of the mortar joints.
3. The diagonal strut model will be adequate to model the reinforced system since failure is governed by corner crushing only with no shear failure. The reinforcing effect is accounted for by incorporating design parameter to account for the stiffness, strength, and ductility increase.

Acknowledgement

The work presented herein is part of a study performed at Drexel University under Grant No. CMS-9730646 from the National Science Foundation (NSF); Dr. Shih-Chi Liu is the NSF program director for this research. The results, opinions, and conclusions expressed in this paper are solely those of the authors and do not necessarily reflect those of the NSF.

References

1. Hakam, Z, H. R. (2000) "Retrofit of Hollow Concrete Masonry Infilled Steel Frames Using Glass Fiber Reinforced Plastic Laminates" Ph.D. thesis, *Civil & Architectural Engineering Department, Drexel University*, Philadelphia, June, pp. 517
2. Eldakhakhni, W. W. (2000) "Non-Linear Finite Element Modeling of Concrete Masonry-Infilled Steel Frame," M.Sc. thesis, *Civil & Architectural Engineering Department, Drexel University*, Philadelphia, March, pp. 184
3. El-Dakhakhni, W. W., Elgaaly, M., and Hamid, A.A., (2001) "Finite Element Modeling of Concrete Masonry-Infilled Steel Frame," *9th Canadian Masonry Symposium*, University of New Brunswick, Canada.
4. Hamid, A.A., and Drysdale, R.G. (1980). " Concrete Masonry Under Combined Shear and Compression Along the Mortar Joints." *ACI journal* September-October , pp. 314-320.
5. Paulay, T. and Priestley, M. J. N. (1992) "Seismic Design of Reinforced Concrete and Masonry Buildings," *John Wiley & Sons, Inc*., New York, NY, USA.
6. Shames, I.H., and Cozzarelli, F.A (1992). "Elastic & Inelastic Stress Analysis" *Prentice Hall*, Upper Saddle River, NJ, USA.

Table 1: Summary of Test Results Analysis of Reference [1]

Frame	Configuration	P_u (kN)	K_{in} (kN/mm)	ΔP_u (kN)	ΔK_{in} (kN/mm)
1	Bare (B-1)	28	2.2	———	———
	Infilled (I-1)	95 / 105	55.7	95-4=**91**	55.7-2.2=**53.5**
	Retrofitted (R-1)	220	131.4	220-14=**206**	131.4-2.2=**129.2**
2	Bare (B-2)	280	21.0	———	———
	Infilled (I-2)	260 / 284	91.4	260-150=**110**	91.4-21.0=**70.4**
	Retrofitted (R-2)	270 / 340	175.0	270-50=**220**	175.0-21.0=**154**

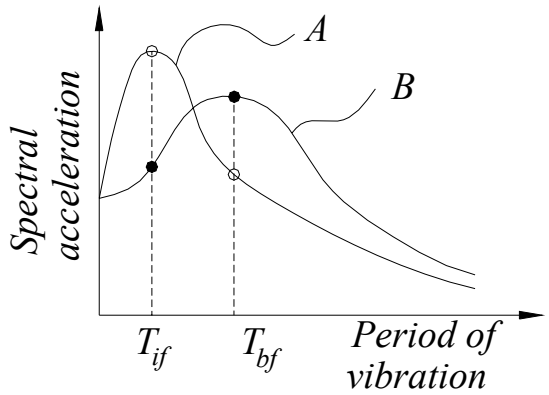

Figure 1. Possible Effects of the Infill Walls Depending on Earthquake Response Spectrum

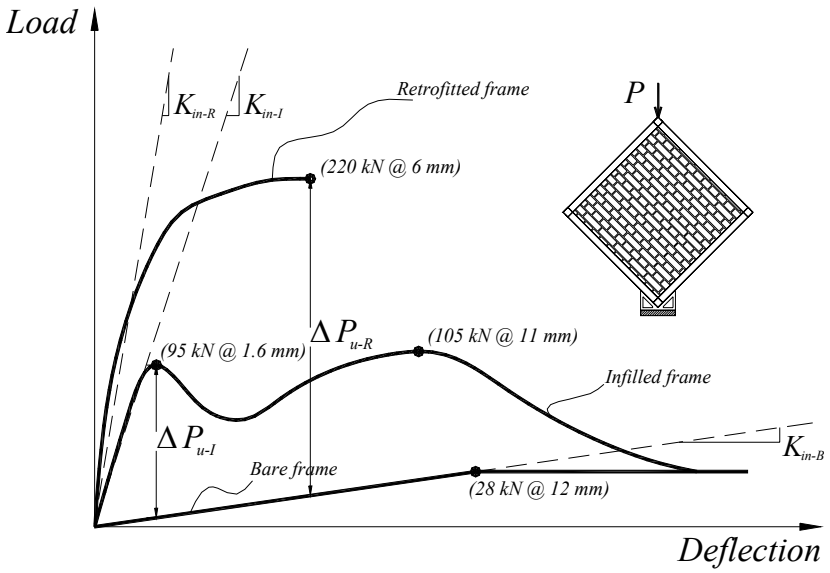

Figure 2. Load-Deflection Relation for Frame 1

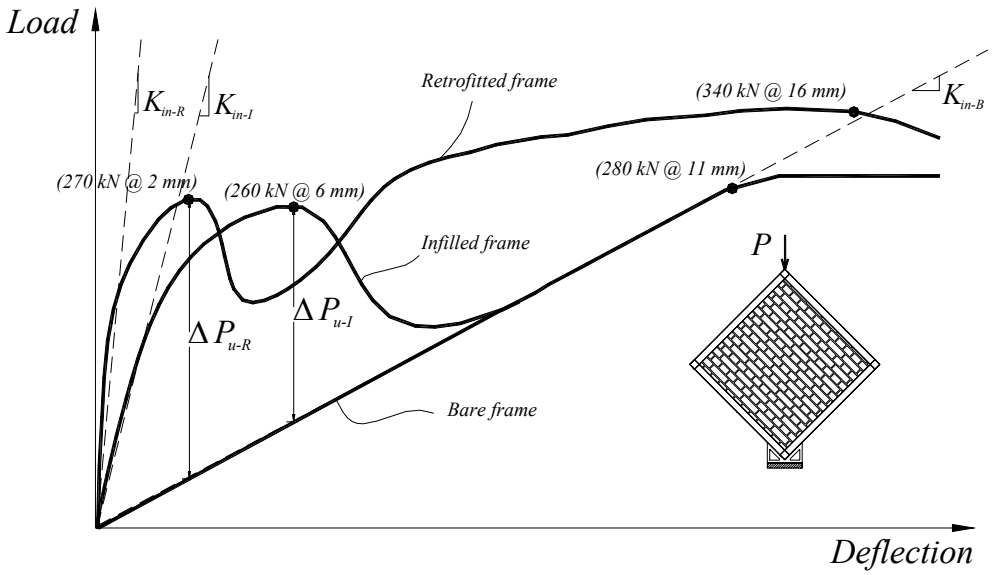

Figure 3. Load-Deflection Relation for Frame 2

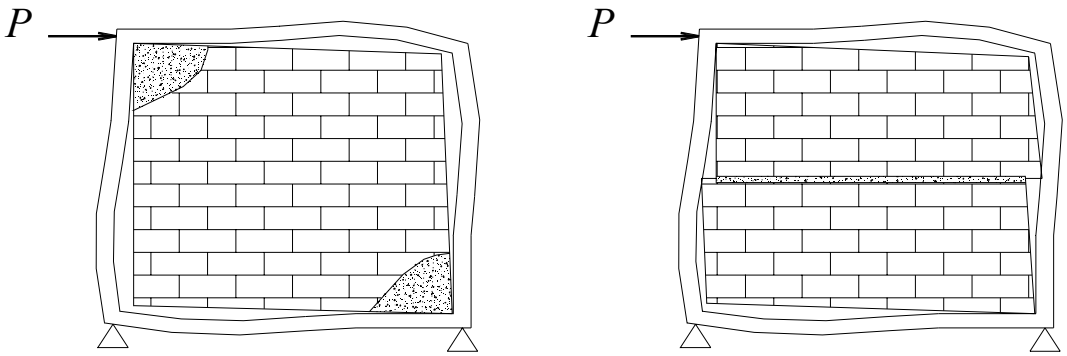

Figure 4. Common Failure Modes: (a) ***C***orner ***C***rushing Mode, (b) ***S***liding ***S***hear Mode

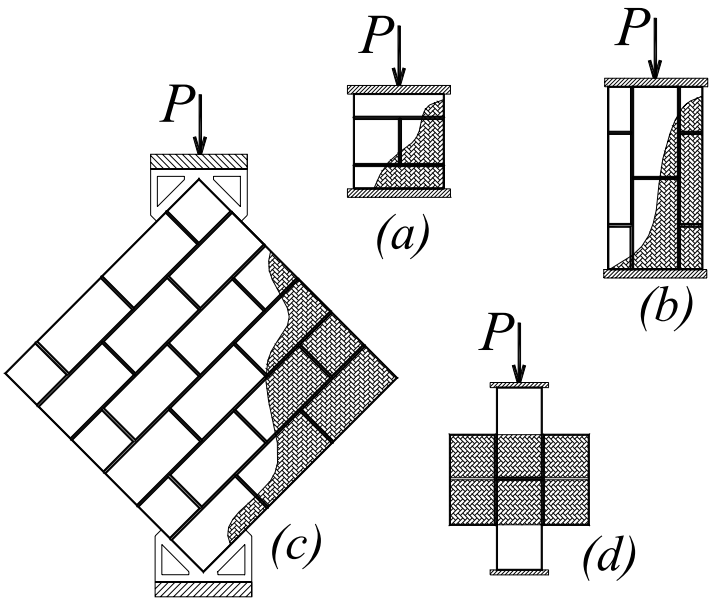

Figure 5. Test Specimens for *Level I* Experiments:
(a) Compression Normal to Bed Joints; (b) Compression Parallel to Bed Joints;
(c) Diagonal Tension; (d) Direct Shear

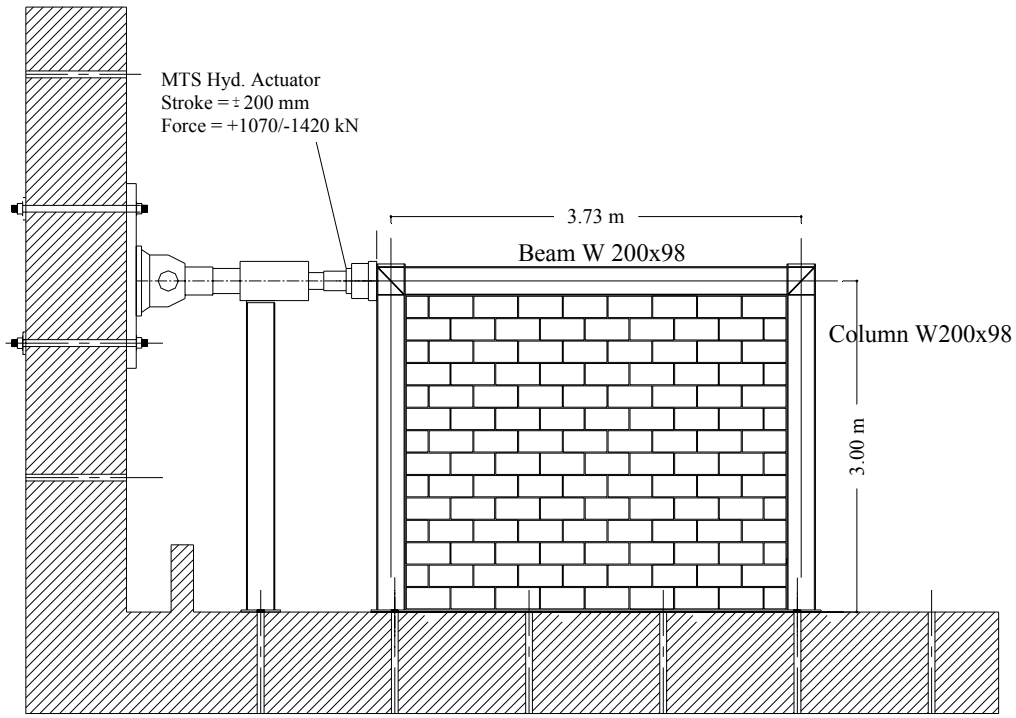

Figure 6. Test Setup for *Level II* Experiments